Discarded sequencing reads uncover natural variation in pest resistance in *Thlaspi arvense*

Dario Galanti[1,2], Jun Hee Jung[1], Caroline Müller[3] and Oliver Bossdorf[1]

[1] Plant Evolutionary Ecology, Institute of Evolution and Ecology, University of Tübingen, 72076 Tübingen, Germany.

[2] Royal Botanic Gardens, Kew, Richmond upon Thames, UK.

[3] Chemical Ecology, Bielefeld University, Universitätststr. 25, 33615 Bielefeld, Germany.

Key words

Aphids, DMRs, DNA methylation, EWAS, glucosinolates, GWAS, mildew, natural variation, pennycress, plant defense

Abstract

Understanding the genomic basis of natural variation in plant pest resistance is an important goal in plant science, but it usually requires large and labour-intensive phenotyping experiments. Here, we explored the possibility that non-target reads from plant DNA sequencing can serve as phenotyping proxies for addressing such questions. We used data from a whole-genome and -epigenome sequencing study of 207 natural lines of field pennycress (*Thlaspi arvense*) that were grown in a common environment and spontaneously colonized by aphids, mildew and other microbes. We found that the numbers of non-target reads assigned to the pest species differed between populations, had significant SNP-based heritability, and were associated with climate of origin and baseline glucosinolates content. Specifically, pennycress lines from cold and thermally fluctuating habitats, presumably less favorable to aphids, showed higher aphid DNA load, i.e. decreased aphid resistance. Genome-wide association analyses identified genetic variants at known defense genes but also novel genomic regions associated with variation in aphid and mildew DNA load. Moreover, we found several differentially methylated regions associated with pathogen loads, in particular differential methylation at transposons and hypomethylation in the promoter of a gene involved in stomatal closure, likely induced by pathogens. Our study provides first insights into the defense mechanisms of *Thlaspi arvense*, a rising crop and model species, and demonstrates that non-target whole genome sequencing reads, usually discarded, can be leveraged to estimate intensities of plant biotic interactions. With rapidly increasing numbers of large sequencing datasets worldwide, this approach should have broad application in fundamental and applied research.

35 **Introduction**

36 Plant pests, such as pathogens and herbivores, can cause major yield losses in crops and often
37 require the massive use of pesticides to control their damage. Natural plant populations, on the
38 other hand, are constantly exposed to such biotic stressors and their higher genetic diversity often
39 allows these populations to become locally adapted. Since many pest species are sensitive to
40 climatic conditions, their pressure on plant communities is spatially heterogeneous, maintaining
41 geographically structured genetic variation in plant defenses (1,2). For these reasons, natural plant
42 populations are highly suitable to study defense mechanisms and evolution of defenses, and also a
43 very useful source of beneficial and resistance alleles for specific pathogens and environmental
44 conditions. This genetic variation in defense-related genes can for example be screened through
45 Genome Wide Association (GWA) (3–6) or approaches based on known candidate genes (2).

46 Many pest species are also highly sensitive to temporal variation in weather conditions. This
47 temporal heterogeneity in pathogen pressure can induce plastic responses in plants, involving gene
48 expression and epigenetic changes (7–9), which may also be studied through stress experiments (7–
49 9). Some plastic epigenetic responses can have a transient stability and be transmitted to the next
50 generations through inheritance of epigenetic marks (10–13). In particular, DNA methylation has
51 been shown to respond to biotic and abiotic stresses through gene expression regulation and
52 transposable elements (TEs) reactivation, and can be inherited across generations (9,12,14). In
53 plants, DNA methylation can occur in the three sequence contexts CG, CHG and CHH (H being A, T or
54 C), which differ in their molecular machineries depositing, maintaining and removing methylation
55 and consequently also in their transgenerational stability (15,16). While CG methylation is usually
56 more stable across generations, CHH methylation is less stable and more responsive to stress and
57 the sensitivity of CHG methylation lies somewhere in between (15–17).

58 Whether inherited or induced, some strategies of plants for defense against pathogens and
59 herbivores include: i) physical barriers such as reinforced cell walls, leaf protective layers or closing
60 stomata, ii) production of specialized (secondary) metabolites that reduce palatability or are toxic to
61 pests, iii) oxidative bursts, iv) the activation of signaling cascades to induce systemic responses and
62 v) RNA interference mechanisms to silence pathogen genes (18–22). In Brassicaceae, a particularly
63 important and diverse class of defense metabolites are glucosinolates, which often show local
64 adaptation driven by variation in pests and can also be induced by herbivore and pathogen attacks
65 (1,2,23).

66 Studying natural variation in plant resistance, along with associated genetic and epigenetic variation,
67 can identify genes involved in defense and their regulators, including vital genes whose function

68 cannot be determined through knockout experiments. Such knowledge, and especially the discovery
69 of natural resistance alleles, are crucial sources for the breeding of more pest-resistant crop
70 varieties. Nevertheless, because of the diversity of resistance mechanisms and their often multigenic
71 nature, plant defense mechanisms remain difficult to study. In particular, antixenosis (the
72 prevention of pathogen settlement) and antibiosis (the repression of pathogen growth and
73 reproduction) require extensive and time-consuming phenotyping, based for example on choice (24)
74 or settling (9) assays, and such assays are extremely challenging to perform on large collections. On
75 the other hand, there are increasing numbers of large sequencing datasets, which may also be used
76 to quantify contaminants or microbiome composition (25–27) and thus as proxies for resistance
77 phenotyping. In this study we investigated such usage of exogenous reads, i.e. reads not mapping to
78 the target reference genome, as a source of information for quantifying herbivore and pathogen
79 abundance in large collections.

80 We worked with field pennycress (*Thlaspi arvense*), an annual plant in the Brassicaceae family that is
81 increasingly studied as a model species (28–32) and new biofuel and winter cover crop (33–36). In a
82 previous study, we investigated natural epigenetic variation in a collection of 207 *Thlaspi* lines from
83 across Europe (32). Prior to their whole-genome and -epigenome sequencing these lines had been
84 grown in a common environment, an open glasshouse where the plants were spontaneously
85 colonized by aphids and powdery mildew, as well as by other microbes. At the time of sequencing,
86 pathogen contamination was still very limited but appeared highly variable, and preliminary analyses
87 showed that it resulted in sizeable amounts of non-target reads assigned to the pest species, i.e.
88 contamination of the DNA samples. Inspired by other recent studies on non-target reads (25–27), we
89 asked if there was systematic variation in the numbers of aphid and pathogen reads among different
90 *T. arvense* lines, and whether these data, together with our whole-genome plant sequencing data,
91 could provide insights into the genomic basis of plant resistance variation.

92 The goals of our study were thus two-fold: i) to contribute to a mechanistic understanding of pest
93 resistance in *Thlaspi arvense*, and ii) to explore whether non-target reads from plant sequencing can
94 be used as proxies for studying plant biotic interactions. Considering that we are moving towards an
95 increasingly sequencing-prone world, with more and larger datasets being generated for many
96 species (37–43), the use of non-target reads has very broad potential.

97

98

99

100 **Results**

101 *Reads classification and species identification*

102 Starting from our previously published sequencing data (32), the first step of our analysis was to
103 separate the Whole Genome Sequencing (WGS) reads of each sample into the ~99.5% mapping to
104 the *Thlaspi arvense* reference genome (29) and the ~0.5% that did not, hereafter called "exogenous
105 reads" (Fig 1A). Initially, we used all mapped reads for calling variants in *Thlaspi*, but after some
106 difficulties with Genome Wide Associations (see below) we suspected that some plant reads were
107 false and mapped to the *T. arvense* genome only because of the high cross-taxa similarity of some
108 genomic regions. We therefore remapped all reads to the genomes of the aphid *Acyrthosiphon*
109 *pisum*, its endosymbiont *Buchnera aphidicola* and the powdery mildew *Blumeria graminis*, and
110 found that, on average, 7.4% of the reads mapped to both *T. arvense* and at least one of the pests.
111 We removed these ambiguous reads from our analyses and used only the *T. arvense* target reads,
112 92.1% on average, for variant calling (Fig 1A, S1 Table).

113 We next attempted a taxonomic classification of the exogenous reads, in multiple steps. First, we
114 used MG-RAST (44,45) to assign reads to taxonomic groups based on public sequencing databases.
115 Out of the 78% of the exogenous reads that passed the MG-RAST quality control (S1 Table) the
116 majority belonged to bacteria and smaller fractions to fungi, plants and animals (Fig 1B and S2
117 Table). For subsequent group-level analyses, we then focused on nine taxonomic groups that
118 occurred consistently within our samples (Fig 1C), and that were particularly abundant or relevant:
119 Erysiphales (fungi), Peronosporales (oomycetes), Aphididae and Culicidae (both insects), and five
120 bacterial families.

121 Visual inspection (Fig 1D) and other sources of information narrowed down the observed aphid and
122 mildew species to a few candidates. For aphids we considered *Acyrthosiphon pisum* (indicated by
123 MG-RAST), *Myzus persicae* (visual match, and a generalist attacking Brassicaceae (46)) and
124 *Brevicoryne brassicae* (attacks Brassicaceae including *Thlaspi* (47)). For powdery mildew we
125 considered *Blumeria graminis* (indicated by MG-RAST), and *Erysiphe cruciferarum* (attacks
126 Brassicaceae (48)). To decide among these species, we then used a competitive mapping approach
127 (49), where the exogenous reads were aligned to a pseudo-reference composed of the same DNA
128 sequences from the different candidate species (see Methods for details, S3 and S4 Tables). The
129 majority (77%) of the aphid reads mapped to *M. persicae*, 18% to *B. brassicae*, and 5% to *A. pisum*,
130 while 98% of the mildew reads mapped to *E. cruciferarum*, with only 2% to the other mildew species
131 (S5 Table). Based on these results, we concluded that the plants in our experiment had been
132 attacked by *Myzus persicae* and *Erysiphe cruciferarum*.

133 Finally, to compare the power of a large database approach (MG-RAST) versus using specific
134 reference genomes, we also remapped all exogenous reads to the *M. persicae* and *B. aphidicola*
135 genome assemblies (50) (www.ncbi.nlm.nih.gov/assembly/GCA_001939165.1) and used the counts
136 from these two mappings as additional phenotypes, besides the nine taxonomic groups selected
137 through MG-RAST (Table 1, S6 Table).

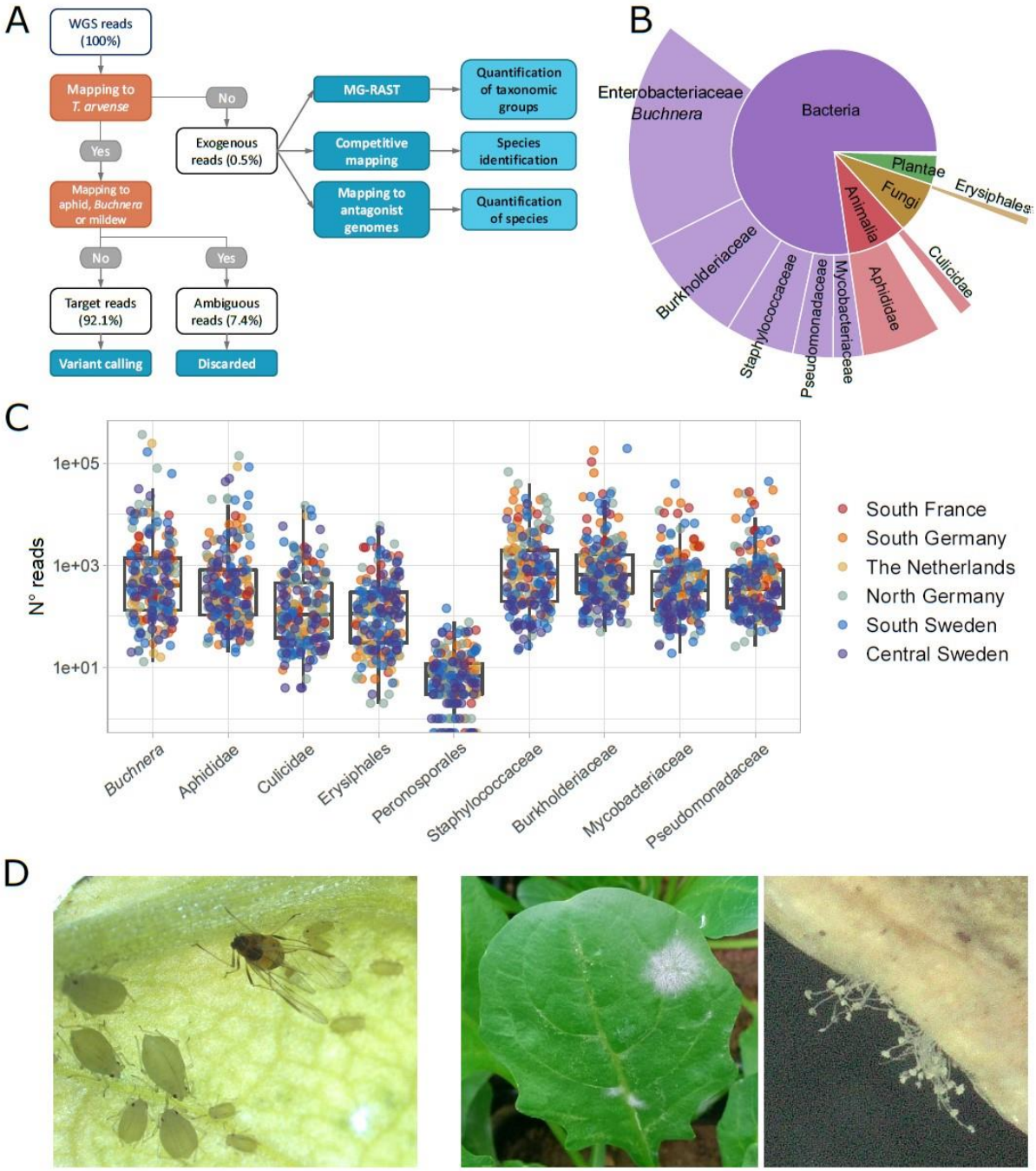

138

139 **Fig 1. Classification of sequencing reads in *Thlaspi arvense* WGS data.** (A) Workflow of the analyses, including reads
140 classification (orange nodes) into target, ambiguous and exogenous reads, and downstream analysis (dark blue nodes) (see
141 Methods). (B) Fractions of exogenous reads assigned to different taxonomic groups by MG-RAST (44,45). (C) Read counts

142 assigned to nine selected groups in our 207 *T. arvense* samples from different European regions. (D) Aphids and mildew
143 occurring on *T. arvense* leaves during our experiment.

144

145 *Exogenous read counts are a heritable Thlaspi phenotype*

146 As we had observed that aphid and mildew infections in the glasshouse were not random, but
147 prevalent on plants from some origins than others, i.e. possibly reflecting heritable variation in plant
148 resistance, we next tested for population differences and SNP-based heritability in pest and
149 microbiome read-counts. Prior to these analyses, to avoid biases caused by different sequencing
150 depths, we corrected the read counts for the total numbers of deduplicated reads in each library and
151 used the residuals as unbiased estimates of aphid, mildew and microbe loads (see Methods).

152 For most of the nine taxonomic groups, there were significant population effects, with 20-40% of the
153 variance in read counts explained, as well as significant SNP-based heritability, typically in the range
154 of 0.18 - 0.30 (Table 1). The highest heritability of 0.47 was for read counts of Erysiphales, indicating
155 particularly strong variation for resistance to mildew. Both SNP-based heritability and population
156 differences tended to be stronger for aphid and *Buchnera* data based on read mapping to the
157 reference genomes than for those based on MG-RAST, demonstrating that the former method is
158 stronger and thus preferable if high-quality genome assemblies are available.

159 An alternative explanation for different aphid and mildew loads in the greenhouse could be that
160 variation in enemy densities in the field was transmitted to the greenhouse, through maternal carry-
161 over effects, or even as seed contamination. However, we had recorded aphid and mildew
162 occurrence during seed sampling in the field and found no significant differences in the glasshouse
163 between the offspring of plants that had been attacked in the field versus those that had not (S1
164 Fig).

165 **Table 1: Population differences and SNP-based heritability for different types of exogenous read counts.** Population
166 differences were tested with a linear model, SNP-based heritabilities (and their confidence intervals) estimated with the R
167 package *heritability* (51).

Taxonomic group	Data type	Population differences (R^2 and *P*-value)	SNP-based heritability
Myzus persicae	Mapping to reference genome	0.245 (*P* = 0.029)	0.190 (0.055-0.488)
Buchnera aphidicola	Mapping to reference genome	0.256 (*P* = 0.016)	0.169 (0.042-0.490)
Buchnera	MG-RAST - genus	0.223 (*P* = 0.090)	0.115 (0.016-0.505)
Aphididae	MG-RAST - family	0.226 (*P* = 0.082)	0.189 (0.052-0.496)

Culicidae	MG-RAST - family	0.166 (P = 0.519)	0.183 (0.055-0.465)
Erysiphales	MG-RAST - order	0.326 (P < 0.001)	0.468 (0.238-0.712)
Peronosporales	MG-RAST - family	0.253 (P = 0.020)	0.266 (0.096-0.553)
Staphylococcaceae	MG-RAST - family	0.390 (P < 0.001)	0.301 (0.124-0.567)
Burkholderiaceae	MG-RAST - family	0.275 (P = 0.005)	0.256 (0.092-0.538)
Mycobacteriaceae	MG-RAST - family	0.362 (P < 0.001)	0.294 (0.120-0.560)
Pseudomonadaceae	MG-RAST - family	0.273 (P = 0.006)	0.192 (0.052-0.505)

Aphid and mildew loads correlate with climate of origin and glucosinolates content of plants

Having established that our method most likely captured variation in plant resistance, we were interested in the ecological drivers of this variation. As climate is known to be a major influence on many biotic interactions as well as plant defenses (1,52), we correlated the observed read counts with the climates of origin of the plants. We found negative correlations between aphid read counts and several temperature variables, in particular annual minimum temperature (Fig 2A). Aphid read counts were also positively correlated with temperature variability, i.e. the diurnal and annual ranges of temperature (Fig 2A). In other words, plants from warmer and more stable climates had consistently lower levels of aphid infestation in our glasshouse, possibly because these plants had evolved greater resistance under such benign climatic conditions where aphids thrive. We found similar, although weaker patterns, for the number of Erysiphales reads. The other analysed taxonomic groups showed different and often weaker patterns of correlation with climate, except that the read counts of several bacterial groups were positively correlated with annual maximum temperature and in particular diurnal temperature range.

Since glucosinolates are major defense metabolites of Brassicaceae, and their variation could thus be an explanation for variance in plant resistance, we also tested for correlations between the baseline amounts of these metabolites and the frequencies of aphid and mildew reads. Glucosinolate levels were measured on the same *T. arvense* lines in a separate experiment not affected by pests (S7 Table). We found positive correlations of aphid read counts with sinigrin, an aliphatic glucosinolate which is by far the most abundant in the leaves of *T. arvense*, and a stronger negative correlation with benzyl glucosinolates (glucotropaeolin) (Fig 2B). Although the baseline levels of benzyl glucosinolates were very low and probably sometimes below the detection level, plant lines where benzyl glucosinolate was detected had significantly lower aphid loads in the glasshouse (Fig 2C). We also detected three indole glucosinolates, but these did not show any significant correlations with aphid loads.

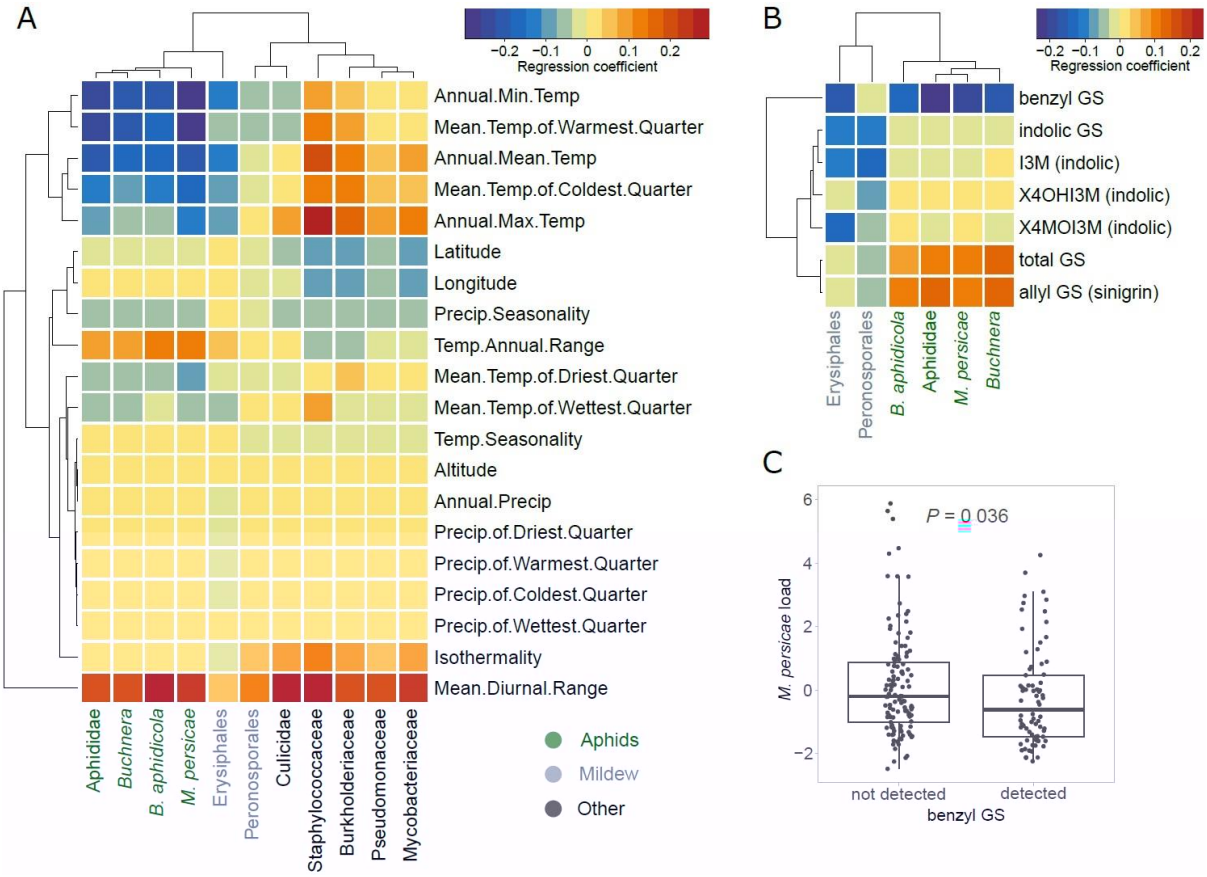

Fig 2. Relationships between climates of origin or glucosinolate levels of plants and the exogenous reads loads. (A) Correlations with bioclimatic variables. (B) Correlations with baseline glucosinolate (GS) levels measured in the same pennycress lines in another experiment. All correlations in (A) and (B) were done after correction for population structure. Aphid-related read counts are in green, mildew-related in gray, others in black. (C) Boxplot of the aphid reads residuals in samples where benzyl GS was detected vs. not. The *P* value is based on the Welch's *t*-test for unequal variances.

GWA identifies peaks near defense genes

To further investigate the genetic basis of variation in aphid, mildew and microbe loads, we next employed GWA and tested for associations between exogenous read counts and biallelic genetic variants (SNPs and short INDELs). We corrected for population structure using an IBS matrix and only tested variants with Minor Allele Frequency (MAF) > 0.04 (see Methods). Initially, we called genetic variants using all reads that mapped to the *T. arvense* genome and found massive peaks in some highly conserved regions of the genome, which had very high mapping coverage (S2 Fig). We suspected that this might be because some non-*Thlaspi* reads were very similar to these highly conserved regions and, by mapping there, generated false variants only in samples containing many non-*Thlaspi* reads. We therefore identified and removed ambiguous reads prior to variant calling,

211 which eliminated the observed massive GWA peaks, indicating that they had indeed reflected false
212 associations (S2 Fig).

213 After excluding the ambiguous reads, we still found significant GWA peaks for Erysiphales but not for
214 other types of exogenous reads (excluding isolated, unreliable variants) (Fig 3A and S3 Fig).
215 Nevertheless, when clear peaks were visible, regardless of their significance, they were usually
216 located close to genes involved in plant defense response. An enrichment analysis (53) confirmed
217 that stronger variants were indeed enriched close to these defense genes (S8 Table) for some
218 exogenous read counts (Fig 3B and S3 Fig). For *M. persicae* load there was a peak in the proximity of
219 *Tarvense_01930*, encoding a predicted pathogenesis-related peptide. The top variant in this peak
220 had a slight but clear allelic effect on *M. persicae* load (Fig 3C). For Erysiphales load we detected a
221 more persistent enrichment, with a highly significant peak in Scaffold 1, located in a region with
222 several defense genes, including *MAJOR LATEX PROTEINS (MLP)* and two genes similar to
223 *Arabidopsis thaliana SALICYLATE METHYLTRANSFERASE 1 (BSMT1)* (Fig 3D and E). This region is wide
224 due to ancient TE colonization, but the top variants are clearly neighboring candidate genes involved
225 in defense (Fig 3E). Other significant peaks for Erysiphales load were close to other genes that
226 possibly contribute to resistance such as *PBL7*, involved in signaling and stomatal closure or *SRF3*,
227 reinforcing cell walls by callose deposition.

228

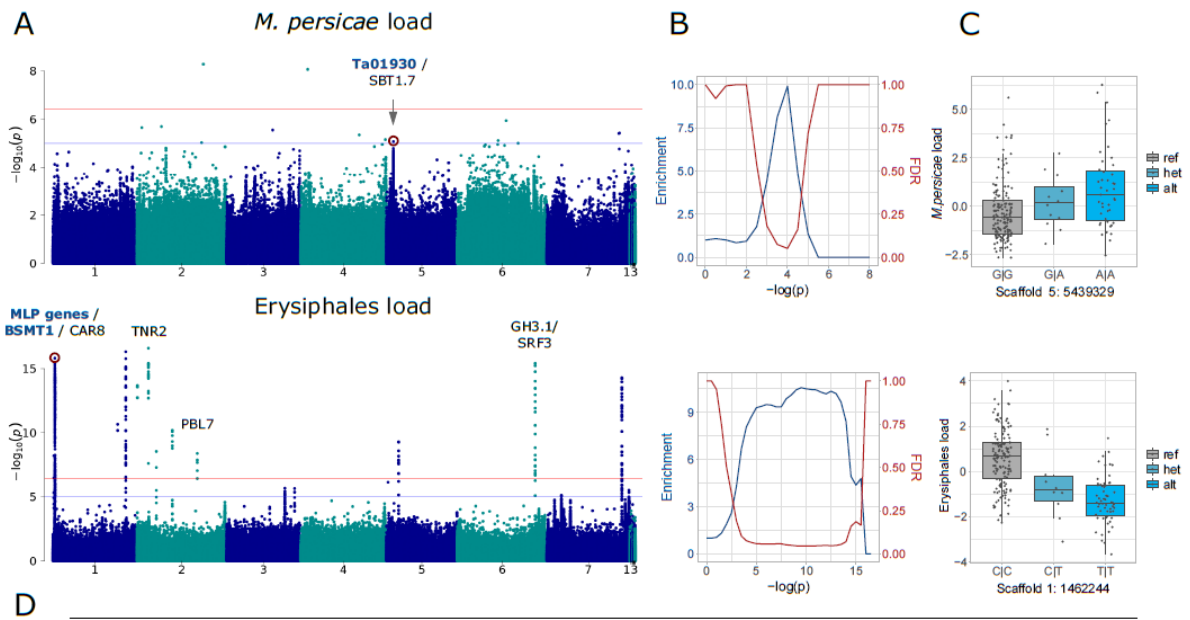

D

Gene name	Gene ID	Ortholog	Putative function	Top SNP location
MLP 31	Ta_10442/45/55	AT1G70840	MAJOR LATEX PROTEIN 31 – Defense response	8 / 2kb downstream
MLP 28	Ta_10443/54	AT1G70830	MAJOR LATEX PROTEIN 28 – Defense response	6 / 1kb downstream
MLP 43	Ta_10444	AT1G70890	MAJOR LATEX PROTEIN 43 – Defense response	4kb downstream
MLP 165	Ta_10446	AT1G35260	MAJOR LATEX PROTEIN 165 – Defense response, GS biosynthesis	< 1kb downstream
BSMT1	Ta_10447/48	AT3G11480	Salicylate/benzoate methyltransferase – Defense response	0kb
CAR8	Ta_10449/53	AT1G23140	Abscisic acid-activated signaling pathway	0 / 2 kb upstream
TNR2	Ta_13332	AT5G46700	Root and epidermis development	1kb downstream
PBL7	Ta_12648	AT5G02800	Brassinosteroid signalling pathway, stomatal closure.	1 kb upstream
Ta01930	Ta_01930	AT3G50020	Predicted PR (pathogenesis-related) peptide – Defense response	12 kb downstream
SBT1.7	Ta_01928/29	AT5G67360	Serine protease essential for mucilage release from seed coats	< 1kb upstream
GH3.1	Ta_05347	AT2G14960	Similar to IAA-amido synthases – Auxine response	< 1kb downstream
SRF3	Ta_05348	AT4G03390	SR FAMILY 3 – Cell wall callose deposition and stress response	3kb upstream

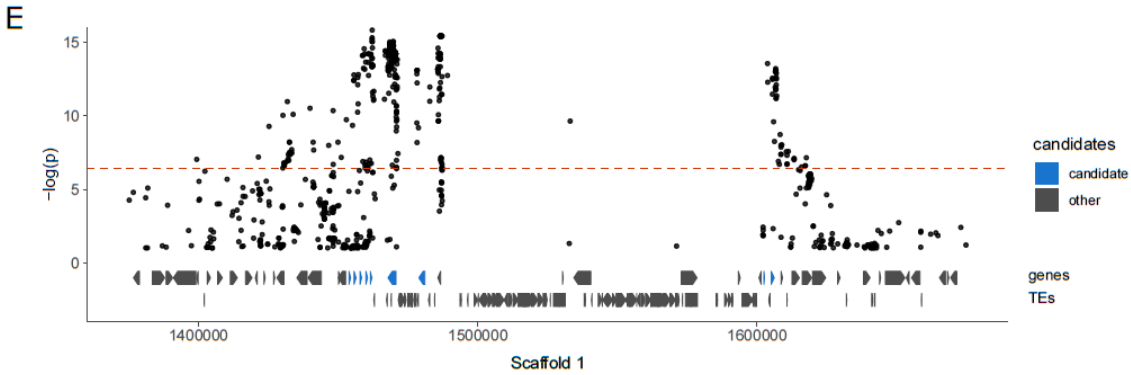

Fig 3. Genome-wide association analyses for aphid and mildew loads. We show only the results for *M. persicae* and MG-RAST Erysiphales read-counts; for full results see S3 Fig. (A) Manhattan plots, annotated with genes potentially affecting aphid/mildew colonization. The genome-wide significance (horizontal red line) was calculated based on unlinked variants (54), the blue line corresponds to –log(p) = 5. (B) Corresponding to the Manhattan plots on the left, enrichment of *a priori* candidates and expected false discovery rates (as in (53)) for increasing significance thresholds. (C) Allelic effects of the red-marked variants in the corresponding Manhattan plots, with genotypes on the x-axes and the read-count residuals on the y-axes. (D) The candidate genes marked in panel A, their putative functions and distances to the top variant of the neighboring peak. Candidates in dark blue are the *a priori* candidates included in the enrichment analyses and involved in

238 defense response (GO:0006952). GS: glucosinolates. (E) Zoom-in for the Manhattan plot of Erysiphales load, around the
239 first peak in Scaffold 1, with gene and TE models below, and *a priori* candidates in blue.

240

241 *Aphid and mildew loads correlate with differential methylation at genes and transposons*

242 Variation in phenotypes, such as our indirect estimates of pest resistance, may not only be
243 associated with DNA sequence but also with epigenetic changes like DNA methylation. This
244 phenotype-associated epigenetic variation can include both heritable and plastic components. The
245 Whole Genome Bisulfite Sequencing (WGBS) data from our previous study (32) allowed us to also
246 explore these questions and to test for associations between DNA methylation variation and pest
247 attack. For simplicity, we limited this analysis to *M. persicae* and Erysiphales loads.

248 Our analysis had two steps: First we called Differentially Methylated Regions (DMRs) between the 20
249 samples with the most and 20 samples with the least *M. persicae* or Erysiphales loads, and then we
250 conducted Epigenome Wide Association (EWA) analyses on individual positions located within these
251 DMRs, using the complete dataset (188 lines - see Methods). This approach allowed us to target
252 genomic regions of interest, while strongly reducing the multiple-testing problem of millions of
253 cytosines in the whole genome and correcting for population structure. Using a relaxed False
254 Discovery Rate (FDR) of 20%, we identified 162 DMRs for *M. persicae* load and 548 DMRs for
255 Erysiphales load (S4 Fig, S9 and S10 Table). The majority of these were in the CG context, especially
256 for *M. persicae*-related DMRs (Fig 4A and S4 Fig). As observed previously (32), DMRs in CHH were
257 generally shorter than in the other sequence contexts (S4A Fig). Since the genome of *T. arvense* is
258 rich in TEs and intergenic regions, the majority of DMRs were located in those features (S4B Fig).
259 However, the DMR density was higher in proximity of genes and particularly in coding sequences (Fig
260 4A), and even DMRs assigned as intergenic (Fig 4A) were often located close to genes or promoters.
261 In accordance with previous studies (8,9), most DMRs were hypomethylated in the infested samples
262 (higher pathogen load), indicating that genes needed for defense might be activated through
263 demethylation.

264 For a more detailed investigation, we turned to EWA, leveraging the power of the entire *Thlaspi*
265 collection. We tested for associations between *M. persicae* or Erysiphales loads and the methylation
266 at individual cytosines located within the DMRs. As in GWA, we corrected for population structure
267 using an IBS matrix. For both types of pest loads, we found associations in the proximity of genes
268 and especially within TEs, but no genomic feature was particularly enriched for low *P*-value
269 associations (S5A Fig). *M. persicae* load was associated with methylation at several genomic
270 locations, especially TEs (Fig 4B), but these associations had strongly inflated *P*-values (S5B Fig). For

271 Erysiphales load the *P*-value distribution was more well-behaved (S5B Fig), and we found a clear
272 association with hypomethylation of Copia family 202 TEs upstream of *MAPKK KINASE 20*
273 (*MAPKKK20*), a gene involved in abscisic acid (ABA) stress response and stomatal closure (Fig 4B, C
274 and D). A coverage analysis confirmed that none of the *T. arvense* lines carries insertions or deletions
275 of the TEs upstream of *MAPKKK20*.

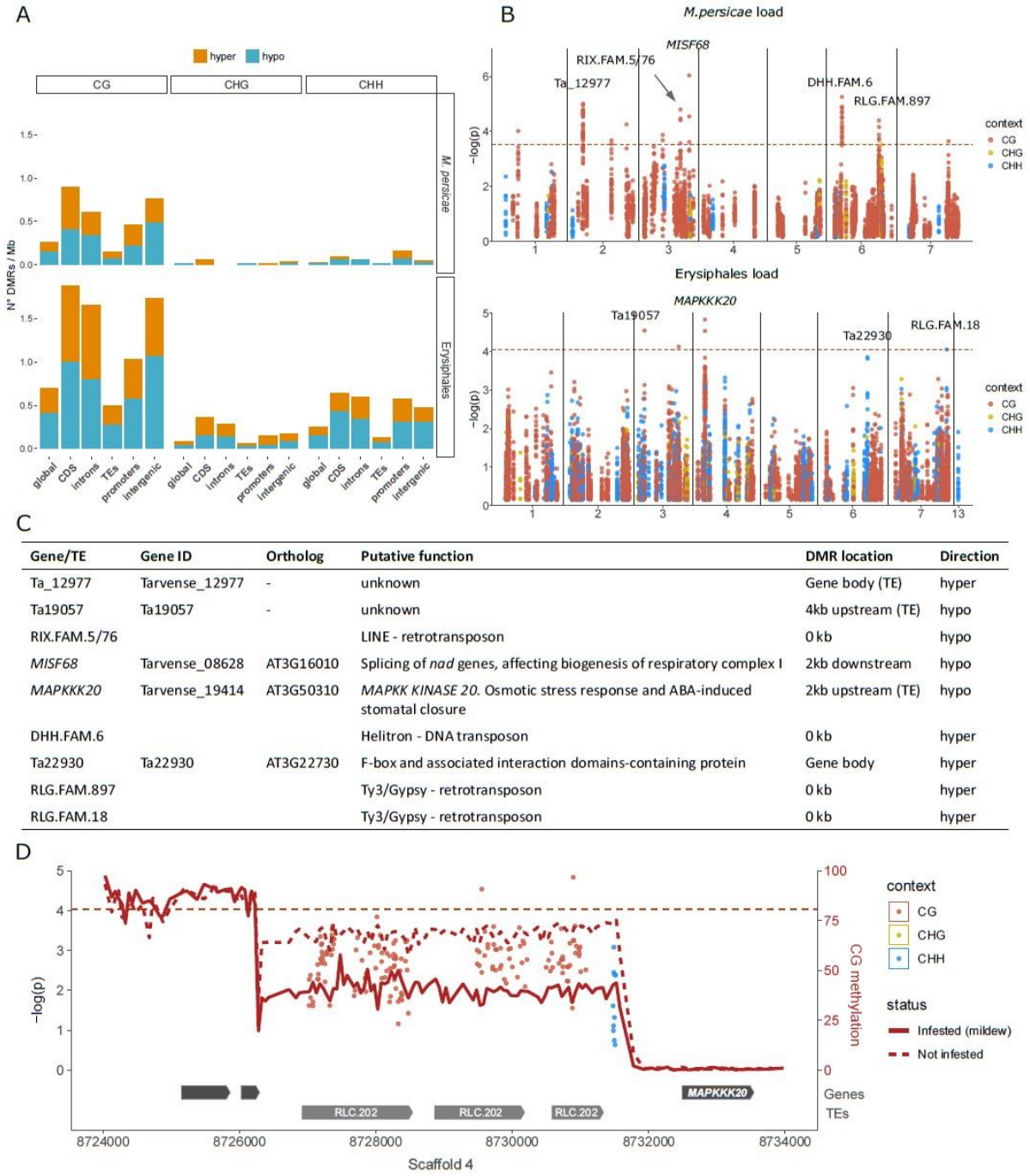

Gene/TE	Gene ID	Ortholog	Putative function	DMR location	Direction
Ta_12977	Tarvense_12977	-	unknown	Gene body (TE)	hyper
Ta19057	Ta19057	-	unknown	4kb upstream (TE)	hypo
RIX.FAM.5/76			LINE - retrotransposon	0 kb	hypo
MISF68	Tarvense_08628	AT3G16010	Splicing of *nad* genes, affecting biogenesis of respiratory complex I	2kb downstream	hypo
MAPKKK20	Tarvense_19414	AT3G50310	*MAPKK KINASE 20.* Osmotic stress response and ABA-induced stomatal closure	2kb upstream (TE)	hypo
DHH.FAM.6			Helitron - DNA transposon	0 kb	hyper
Ta22930	Ta22930	AT3G22730	F-box and associated interaction domains-containing protein	Gene body	hyper
RLG.FAM.897			Ty3/Gypsy - retrotransposon	0 kb	hyper
RLG.FAM.18			Ty3/Gypsy - retrotransposon	0 kb	hyper

276

277 **Fig 4. Differential methylation associated with aphid and mildew loads.** (A) Differentially Methylated Region (DMR)
278 densities in different genomic features when comparing the 20 samples with the most vs. the least *M. persicae* (top) or
279 Erysiphales (bottom) load. CDS: coding sequences. (B) Manhattan plots from EWA analyses based on individual cytosines
280 within DMRs, with sequence contexts in different colours and annotation of genes close to low *P*-value cytosines. The

genome-wide Bonferroni significance thresholds (dashed red lines) were calculated based on the number of DMRs. (C) Candidate genes and TEs marked in panel B, their putative functions, genomic locations of associated DMRs, and whether infested samples were hyper- or hypomethylated. (D) Zoomed-in Manhattan plot for Erysiphales load around the peak in Scaffold 4, with gene and TE models given below. The CG methylation in the 20 most and least infested samples was calculated over 50 bp bins (see S5C Fig for methylation in other contexts).

Discussion

Plant pests are a major threat to food safety, causing large yield losses, and new crops such as the potential biofuel plant *Thlaspi arvense* must be able to resist pathogen and herbivore attacks. A powerful source for obtaining resistant varieties is natural variation in plant defenses, but phenotyping large collections can be very time-consuming and error-prone. Here we describe how an unplanned pest infestation in a glasshouse experiment, together with available WGS data, can be used to estimate aphid, mildew and microbial loads, and thus variation in plant resistance. The approach is straightforward, makes use of WGS data without microbiome-specific DNA extraction, and can in principle be applied to many other situations such as field experiments. It is not error-free, but we highlight some potential pitfalls, show how to reduce noise, and illustrate its potential to detect associations with climatic, genetic and epigenetic variation.

An important first step in our analyses was the identification and classification of pest-related reads in the plant WGS data. We began by classifying all reads as target (only mapping to *T. arvense*), ambiguous (mapping to *T. arvense* and at the same time to at least one of the pest genomes) or exogenous (not mapping to *T. arvense*) (Fig 1A). We demonstrated the importance of removing ambiguous reads prior to variant calling, as this prevented calling false positive variants caused by exogenous DNA that also mapped to highly conserved or repetitive sequences in the *T. arvense* genome. We then classified the exogenous reads using MG-RAST (44,45) or by confident mapping to specific pest genomes, and selected the eleven most relevant and/or abundant taxonomic groups to focus our analyses on. To obtain unbiased pest/microbe loads we also corrected the read-counts for the total number of deduplicated reads of each sample. A competitive mapping approach allowed us to identify the aphid and mildew species that had occurred in our experiment as the generalist aphid *Myzus persicae* and the powdery mildew *Erysiphe cruciferaum* (Fig 2).

Since we suspected a non-random colonization of pests and microbes in our *T. arvense* collection, we tested for population differences as well as SNP-based heritability. We found significant population differences for most pest and microbe loads, and often heritabilities above 15%, which although low, is still indicative of genetic determination (5). Moreover, Erysiphales load had a

314 particularly high heritability of 47% (Table 1). We therefore next asked what could explain the
315 observed variation in pest loads in our experiment. As pathogen abundances in the field are often
316 determined by climatic conditions, we expected plants originating from climates less favorable to
317 aphids to perform worse in our glasshouse, i.e. to have higher pathogen loads. As expected, aphid
318 counts were negatively correlated with temperature of origin (particularly minimum temperature),
319 and positively with temperature variability (Mean Diurnal Range and Temperature Annual Range)
320 (Fig 3A), suggesting that plants from colder and more thermally fluctuating climates, which are less
321 favorable to aphids, were less well defended and performed worse in our glasshouse. We found
322 similar but weaker patterns for Erysiphales load.

323 As we expected the observed climate-associated variation in pest loads to be at least partially
324 explained by variation in chemical defenses, and since in *Arabidopsis thaliana* glucosinolates, the
325 main defensive compounds, are known to be geographically structured in response to aphid
326 distributions (1), we also tested for association of aphid and mildew loads with glucosinolates in our
327 collection. In accordance with literature on *A. thaliana* (55), we observed a positive correlation of
328 aphid loads with total glucosinolates as well as with the most abundant glucosinolate sinigrin
329 (aliphatic glucosinolate), but a negative correlation with benzyl glucosinolates (Fig 3B). These
330 findings suggest that glucosinolate composition, rather than total amount, is important for aphid
331 defense, and that while benzyl glucosinolates might have a deterrent effect, sinigrin might on the
332 contrary attract *M. persicae* or act as a stimulant, which would be in accordance with previous
333 observations (56).

334 To detect genetic variants associated with pest and microbe loads, we then conducted a GWA study.
335 For aphid (*M. persicae*) load, we detected only one non-significant peak in Scaffold 5, close to a
336 pathogenesis-related coding gene (Fig 3A and D). For Erysiphales load, however, there were several
337 significant associations neighboring genes directly involved in defense, mostly members of the *MLP*
338 family, clustered in a large peak on the first arm of Scaffold 1 (Fig 3E). *MLP165*, the closest gene to
339 the most significant variant in the peak, is indirectly involved in GS biosynthesis in *A. thaliana* (57),
340 which might explain why baseline GS levels were associated with Erysiphales load (Fig 3B). Further
341 GWA peaks for Erysiphales pointed towards other genes indirectly involved in the defense response
342 through phytohormone signaling (eg. *CAR8, PBL7, GH3.1*) or preventing pathogen access through
343 cell wall reinforcement or stomatal closure (*SRF3, PBL7*) (Fig 3D). Further experiments would be
344 necessary to confirm the functionality of these genes.

345 An important general insight from our GWA analyses was the frequent ambiguity of reads that
346 mapped to both pest and host plant genome. Such ambiguous reads generated false variants only

347 present in samples with pest DNA, which resulted in highly significant false associations, and it was
348 therefore important to remove these reads before variant calling. Another potential reason for
349 sequence similarity between host and pathogens could be defense mechanisms such as RNA
350 interference. If *T. arvense* produces small or micro RNAs to silence pathogen genes, this would
351 originate from genomic regions of high similarity between host and pathogen, and thus reflect a true
352 association. However, a BLAST (58) of the region in which the suspicious associations occurred did
353 not reveal any similarity to aphid or mildew genes, but instead to the highly conserved ribosomal
354 RNA coding regions. While genetic variants are generally inherited from parents and thus reflect
355 evolutionary processes, DNA methylation variants can be heritable but can also reflect plastic
356 responses to environmental stresses like herbivores or pathogens. Our data do not allow to
357 confidently distinguish between these two sources of DNA methylation variation, and thus should be
358 interpreted with caution, especially with regard to the directionality of associations. A beneficial
359 DNA methylation variant is expected to be associated with lower pathogen load when already
360 present before pathogen arrival, but with higher pathogen load when plastically induced by
361 pathogens during the experiment. For both *M. persicae* and Erysiphales, the majority of DMRs were
362 hypomethylated in affected samples, which is in accordance with the loss of methylation observed in
363 *A. thaliana* and *T. arvense* upon aphid feeding, and in diploid wheat upon powdery mildew infection
364 (8,9,31), but we also detected hypermethylation at several loci. *M. persicae* load was associated with
365 differential methylation at only few genes but several TEs, which is in accordance with the aphid or
366 stress-induced TE reactivation observed in *A. thaliana* (9,14). Erysiphales load was associated with
367 hypomethylated Copia TEs upstream of *MAPKKK20*, a gene involved in ABA-mediated signaling and
368 stomatal closure. Since stomatal closure is a known defense mechanism to block pathogen access
369 (21), it is tempting to conclude that hypomethylation of the *MAPKKK20* promoter might induce its
370 overexpression and consequent stomatal closure, thereby preventing mildew access to the leaf
371 blade. Overall, we found associations between pathogen load and TE methylation that could
372 potentially act both in *cis* (eg. Copia TE methylation in *MAPKKK20* promoter) and in *trans*, for
373 example through transposon reactivation (eg. LINE, Helitron and Ty3/Gypsi TEs isolated from genes).
374 Although we cannot confidently distinguish inherited versus induced DNA methylation variants, to
375 our knowledge this is the first coupled GWA - EWA analysis conducted on a large natural plant
376 collection.

377 In summary, our study offers first insights into the defense mechanisms of *Thlaspi arvense*, including
378 candidate genes and alleles which may be of interest for breeding efforts in this novel biofuel and
379 cover crop. It also provides a proof of principle that exogenous reads from large sequencing efforts,
380 usually discarded if not mapping to the target genome, can be leveraged to extract additional

381 information about important biotic interactions of the target species, including its antagonists and
382 microbiome components. We combined this approach with data from a common environment
383 experiment to show that pest and microbiome load were geographically structured, as expected
384 from locally adapted traits, and associated with both genetic and DNA methylation variants. In
385 principle, our approach can be applied to many other designs. For example, field-collected samples
386 could be used to quantify geographic pathogen distributions. With the decreasing cost of sequencing
387 and increasing large-scale and single-species sequencing projects e.g. (37–43), the number of data-
388 sets suitable for such analyses is set to rapidly increase in the near future.

389

390 **Materials and Methods**

391 *Plant growth and sequencing*

392 The WGS data used in this study were already published in Galanti et al. (2022) (32). Please refer to
393 this publication for details on data generation and methods. Briefly, we collected 207 *Thlaspi*
394 *arvense* accessions from 36 European populations in July 2018, and we grew their offspring in a
395 glasshouse at University of Tübingen (48°32'21.3"N, 9°02'04.2"E) between August and October 2019.
396 The glasshouse was located in biodiverse surroundings, and insects and pests could enter when the
397 windows opened for temperature regulation. A few weeks after germination, we noticed aphid and
398 mildew infestations. After 46 d we sampled the 3rd or 4th true leaf of each plant and snap-froze it in
399 liquid nitrogen. We extracted DNA using the DNeasy Plant Mini Kit (Qiagen, Hilden, DE), sonicated
400 (Covaris) 300 ng of genomic DNA and used the NEBNext Ultra II DNA Library Prep Kit for Illumina
401 (New England Biolabs) to prepare the libraries. Half way through the protocol we split the DNA into
402 1/3 for genomic libraries and 2/3 for bisulfite libraries. For the bisulfite conversion we used the EZ-
403 96 DNA Methylation-Gold MagPrep (ZYMO) kit. We sequenced paired-end for 150 cycles using
404 Illumina NovaSeq 6000 (Illumina, San Diego, CA) for genomic libraries and HiSeq X Ten (Illumina, San
405 Diego, CA) for bisulfite libraries.

406

407 *Reads mapping and classification*

408 Upon demultiplexing the raw reads, we used cutadapt (59) for quality (minimum quality of 20) and
409 adaptor trimming, excluding reads shorter than 35 bp. We used FastQC and MultiQC (60,61) to
410 estimate the duplication rate, and calculated the total deduplicated reads, which we later used for
411 correcting the number of exogenous reads. We then classified the reads based on their mapping
412 behavior. First we aligned reads to the *T. arvense* reference genome (29) with BWA-MEM v0.7.17

413 (62), excluding multimapping reads (-c 1) and marking duplicates with MarkDuplicatesSpark (63,64).
414 We then mapped all samples again (62) to the three putative exogenous genomes of pea aphid
415 (*Acrophyson pisum*), the aphid symbiont *Buchnera aphidicola* and powdery mildew (*Blumeria*
416 *graminis*), using available resources (www.ncbi.nlm.nih.gov/assembly/GCF_005508785.2,
417 www.ncbi.nlm.nih.gov/assembly/GCA_001939165.1) (65). After this, we used a custom script to
418 collect all read IDs within a sample mapping to any of the three exogenous genomes, and removed
419 any of these reads from the *T. arvense* alignment bam files. We thus removed all ambiguous reads
420 before proceeding with variant calling. To compare coverage of specific regions with and without
421 ambiguous reads, we used samtools bedcov (67). The numbers of reads classified by their mapping
422 behaviour are reported in S1 Table.

423

424 *Variant calling*

425 For variant calling we used GATK4 v4.1.8.1 (63,64), following the best practices for germline short
426 variant discovery (https://gatk.broadinstitute.org/hc/en-us/articles/360035535932-Germline-short-
427 variant-discovery-SNPs-Indels-) with few adjustments for large datasets (32). Briefly, starting from
428 the bam files generated after the removal of ambiguous reads, we i) ran HaplotypeCaller, ii)
429 combined the resulting GVCF files with GenomicsDBImport and GenotypeGVCFs and iii) filtered out
430 low quality variants with VariantFiltration (see Galanti et al. (2022) (32) for more details). Finally, we
431 used vcftools v0.1.16 (67) to retain biallelic variants with MAF > 0.01 and a maximum of 10% missing
432 genotype calls. We imputed these missing calls with BEAGLE 5.1 (68) to obtain a complete
433 multisample vcf file.

434

435 *Identification and classification of exogenous reads*

436 To identify exogenous reads, we extracted all unmapped reads from the bam files created aligning
437 WGS reads to the *T. arvense* genome (29). We selected reads with both mates unmapped (SAM flag
438 12) and excluded supplementary alignments (SAM flag 256 after running MarkDuplicatesSpark) with
439 samtools (65). We then recovered these reads from the trimmed fastq files with seqtk subset
440 (https://github.com/lh3/seqtk) to obtain fastq files of unmapped reads only. We used these as input
441 for MG-RAST (44,45), a web-based tool for phylogenetic analysis of metagenomes.

442 We ran MG-RAST mostly with default parameters, without assembled reads, excluding dereplicated
443 sequences, and dynamically trimming reads with a minimum Phred score of 15 in more than 5
444 consecutive bases. We set the "sequence screening" to *A. thaliana*, the closest relative of *T. arvense*

445 available. We used two different approaches to extract read counts. First we classified all reads up to
446 family level using the web-based Analysis tool from MG-RAST. We used RefSeq as query annotation
447 database and filtered reads classified with low confidence using default settings: e-value 5, 60 %-
448 identity, length 15 and min.abundance of 1 (S2 Table). Out of the hundreds of taxonomic groups
449 identified by MG-RAST, we selected only a small subset for follow-up analyses, based on their
450 biological relevance, our visual observations and/or abundance: Aphididae, Culicidae,
451 Peronosporales, Staphylocaccaceae, Burkholderiaceae, Mycobacteriaceae and Pseudomonadaceae
452 (Table 1). Additionally, we used a custom Python script to download individual "taxonomy" or
453 "sequence_breakdown" results from MG-RAST API (69) and extracted the counts of the genus
454 *Buchnera,* including bacterial symbionts of many aphid species, and of the order Erysiphales, to
455 quantify the observed mildew infection (Table 1). All the code for extracting counts for all families or
456 specific taxonomic groups are available on GitHub (https://github.com/junhee-jung/MG-RAST-read-
457 counter).

458 In addition to the nine read groups selected from MG-RAST results, we also performed a highly
459 confident mapping of exogenous reads to the *M. persicae* and *B. aphidicola* genome assemblies (50)
460 (www.ncbi.nlm.nih.gov/assembly/GCA_001939165.1), to test whether mapping to a high quality
461 assembly of the exact pathogen has a higher sensitivity than MG-RAST. We mapped with BWA-MEM
462 v0.7.17 (61), using a seed length of 25 bp (70) and removing reads with MAPQ < 20 and duplicates
463 with MarkDuplicatesSpark (63,64). We then counted all reads in the bam files.

464 Finally, we log transformed all read counts to approximate normality, and corrected for the total
465 number of deduplicated reads by extracting residuals from the following linear model,
466 log(read_count + 1) ~ log(deduplicated_reads), which allowed us to quantify non-Thlaspi loads,
467 correcting for the sequencing depth of each sample.

468

469 *Exogenous reads heritability and species identification*

470 To exclude the possibility that aphid and mildew infestation patterns were carried-over from the
471 field, through seed contamination or maternal effects, we used aphid and mildew presence/absence
472 data collected in the field. We found no difference in aphid or mildew loads between samples with
473 and without aphids or mildew on the original parental plant in the field (S1 Fig). Nevertheless, to
474 exclude a possible bias, we excluded one outlier sample with particularly high aphid load and aphids
475 observed in the field (S1 Fig) from the analyses.

476 To test for variation between populations we used a general linear model with population as a
477 predictor. To measure SNP-based heritability, i.e. the proportion of variance explained by kinship,
478 we used the marker_h2() function from the R package *heritability* (51), which uses a genetic distance
479 matrix as predictor to compute REML-estimates of the genetic and residual variance. We used the
480 same IBS matrix as for GWAS and for the correlations with climatic variables.

481 Even though MG-RAST classifies reads based on all taxonomic ranks, the accuracy of species
482 identification of course strongly depends on the sequences available in the query databases. MG-
483 RAST assigned our aphid reads to *A. pisum*, but this did not fit with our visual observations and with
484 the poor performance of this species on Brassicaceae (71). We therefore selected three plausible
485 aphid species and test which of these had mostly likely attacked our experiment. In addition to *A.*
486 *pisum*, we tested two other aphid species commonly attacking Brassicaceae: *Brevicoryne brassicae*
487 and *Myzus persicae*. While not all three species have reference genomes available, all mitochondrial
488 genomes are available on NCBI (72) under accession numbers MN232006, NC_011594 and
489 NC_056270. We downloaded these sequences, aligned them to each other (73), removed INDELs to
490 retain only SNPs and combined them into a single pseudo-reference fasta file (S3 Table). We then
491 mapped the exogenous reads from 40 randomly selected samples to this pseudo-reference, allowing
492 for unique mappings only and counted the reads mapping to either of the three aphid species. We
493 used the same approach for mildew except that we included only two possible species: *Blumeria*
494 *graminis*, as suggested by MG-RAST, and *Erysiphe cruciferarum* which is known to attack
495 Brassicaceae but was not in the MG-RAST query database and seemed plausible from visual
496 inspection (Fig 2B). For the mildew pseudo-reference (S4 Table) we used the Internal Transcribed
497 Spacer (ITS), which is publicly available for both species on NCBI (71) under accession numbers
498 MT644878 and AF031283.

499

500 *Quantification of glucosinolates*

501 Using seed material collected from the sequenced plants, we conducted a follow-up experiment to
502 estimate the glucosinolates (GS) content of all 207 lines in the absence of pathogens. Briefly, we
503 sowed the seeds in petri dishes, stratified them at 4°C in the dark for two weeks and transplanted
504 the germinated seedlings to individual 9 x 9 cm pots. We grew the plants in a growth chamber with a
505 14/10 h light/dark cycle at 21/17 °C and a relative humidity of ~45%. Two weeks after germination
506 the plants were vernalized at 4°C for two more weeks in order to minimize phenological and
507 developmental differences between winter and summer annuals. Ten days after vernalization, we
508 collected the 3rd or 4th true leaf and snap-froze it in liquid nitrogen. After freeze drying, we weighed

509 all samples and extracted the material threefold in 80% methanol, adding *p*-hydroxybenzl
510 glucosinolate (Phytoplan, Heidelberg, Germany) as internal standard. After centrifugation, we
511 applied the supernatants onto ion-exchange columns with diethylaminoethyl (DEAE) Sephadex A25
512 (Sigma Aldrich, St.Louis, MO, USA) in 0.5 M acetic acid buffer, pH 5. We added purified sulfatase,
513 converting glucosinolates to desulfo glucosinolates. After one day, we eluted desulfo glucosinolates
514 in water and analyzed them on a HPLC coupled to a DAD detector (HPLC-1200 Series, Agilent
515 Trechnologies, Inc., Santa Clara, CA, USA) equipped with a Supelcosil LC 18 column (3 µm, 150×3
516 mm, Supelco, Bellefonte, PA, USA). We analysed the samples with a gradient from water to
517 methanol starting at 5% methanol for 6 min and then increased from 5 to 95% within 13 min with a
518 hold at 95% for 2 min, followed by a column equilibration cycle. We identified different
519 glucosinolates based on their retention times and UV spectra in comparison to respective standards
520 and an in-house database. We integrated peaks at 229 nm and calculated respective glucosinolate
521 concentrations in relation to the internal standard and sample dry mass, using response factors as
522 reported by Agerbirk et al. (2015) (74).

523

524 *Drivers of exogenous reads variation*

525 To test for associations between glucosinolate variation, as well as climate of origin, and the
526 observed pest loads, we extracted average bioclimatic variables for the 25 years predating our
527 experiment for our 36 study populations from the Copernicus website (75), as described in Galanti et
528 al. 2022 (32). We then used the R package *lme4qtl* (76) to run mixed models that included either
529 bioclimatic variables or glucosinolate contents as explanatory variables, and the exogenous read
530 counts as dependent variables, while correcting for population structure with the same IBS matrix as
531 in GWA and EWA analyses (see below).

532

533 *GWA analysis*

534 We conducted GWA with mixed models that corrected for population structure with a genetic
535 Isolation By State (IBS) matrix as a random factor, as implemented in GEMMA (77). To obtain the IBS
536 matrix we used PLINK v 1.90b6.12 (78). Starting from the imputed multisample vcf file obtained from
537 variant calling, we pruned variants with LD > 0.8 in 50 variants windows, sliding by five. To produce
538 the genetic variants used for GWAS, we also started from the imputed multisample vcf file from
539 variant calling and filtered out variants with MAF < 0.04. As phenotypes we used the number of
540 exogenous reads corrected for the total number of deduplicated reads, as described above.

541 To validate our results and test for overlap with existing gene functional annotations, we performed
542 an enrichment analysis of variants neighboring *a priori* candidate genes as described in Atwell et al.
543 (2010) (53). Briefly, we attributed *a priori* candidate status to all variants located within 20 kb from
544 orthologs (79) of *A. thaliana* genes annotated with the GO term "defense response" (GO:0006952),
545 including nine genes similar to *AtBSMT1* (S8 Table). We then calculated enrichment for incremental -
546 log(p) thresholds as the ratio between observed frequency (significant *a priori* candidate / significant
547 variants) and background frequency (total *a priori* candidate / total variants), and an upper bound
548 for the FDR (32,53). We further assessed the significance of the enrichment through a previously
549 established genome rotation scheme (80). Briefly, we calculated a null distribution of enrichments
550 by randomly rotating the *P*-values and *a priori* candidate status of the genetic variants within each
551 chromosome for 1M permutations. We then assessed significance by comparing the observed
552 enrichment at the Bonferroni threshold to the null distribution. The code for these analyses is
553 available on https://github.com/Dario-Galanti/multipheno_GWAS/tree/main/gemmaGWAS.

554

555 *Methylation and DMR calling*

556 For the methylome analyses we used the EpiDiverse toolkit (81), specifically designed for large
557 WGBS datasets. We used the WGBS pipeline (https://github.com/EpiDiverse/wgbs) for read
558 mapping and methylation calling, retained only uniquely-mapping reads longer than 30 bp, and
559 obtained individual-sample bedGraph files for each sequence context. We then called DMRs using
560 the DMR pipeline (79), with a minimum coverage of 4x. We compared the 20 samples with the most
561 and the least *M. periscae* and Eriysiphales loads, resulting in two sets of DMRs for each sequence
562 context. Since this was only the first step of our methylation analysis, meant to identify potential
563 regions of interest, we retained all DMRs with a FDR < 20%. To understand the genomic preferences
564 of DMRs, we intersected them with genomic features and calculated their densities in each by
565 dividing their number by the total Mb covered by each genomic feature in the genome.

566

567 *EWA analysis*

568 Following the DMR calling, we investigated methylation-phenotype relationships in more detail,
569 using EWA. We ran EWA similarly to GWA, enabling the "-notsnp" option available in GEMMA (76),
570 and correcting for population structure with the same IBS matrix. To exclude possible biases, we
571 excluded all samples with a bisulfite non-conversion rate >1 (32), which left 188 samples for analysis.
572 To generate the methylation input files we first used custom scripts (https://github.com/Dario-

573 Galanti/WGBS_downstream/tree/main/WGBS_simpleworkflow) (32) to unite individual-sample
574 bedGraph files into unionbed files and retain positions with coverage > 3 in at least 95% of the
575 samples and a methylation difference of at least 5% in at least two samples. We then intersected the
576 unionbed files with the DMRs of the corresponding sequence context using bedtools (82) and
577 converted unionbed to BIMBAM format as input for GEMMA.

578 We ran EWA for individual positions within the DMRs and calculated Bonferroni thresholds based on
579 the number of DMRs, assuming that cytosines within the same DMR are mostly autocorrelated. To
580 observe in which genomic features associations with lower *P*-values were located, we performed
581 enrichment analyses similar to the ones performed for defense *a priori* candidate genes in GWA (53),
582 but based on whole genomic features. Starting from all cytosines used for EWAS, we calculated the
583 background frequency as the fraction of all cytosines located in each genomic feature and then
584 calculated the observed frequency in the same way for -log(p) 0.5 increments, with enrichment as
585 the ratio of observed and expected frequencies. All code used for EWA and the enrichment analysis
586 in genomic features is available on https://github.com/Dario-
587 Galanti/EWAS/tree/main/gemmaEWAS.

588

589 **Supporting Information**

590 **S1 Fig. Pest loads in samples with or without pests in the field.** Offspring from plants with or
591 without pathogens in the field did not differ (n.s.) in pathogen loads in the glasshouse, suggesting
592 the pathogens were not carried with the seeds. A single outlier (TA_NL_03_04) with aphids in the
593 field also showed high levels of aphid load in the glasshouse and was excluded from the analysis.

594 **S2 Fig. Example of a GWA peak caused by ambiguous reads.** (A) Manhattan plot of GWA with aphid
595 load, without removing ambiguous reads prior to variant calling. The genome-wide significance
596 (horizontal red line) was calculated based on unlinked variants (54), the suggestive line (blue)
597 corresponds to -log(p) =5. (B) Zoomed-in peak on Scaffold 6 with coverage before and after removal
598 of ambiguous reads.

599 **S3 Fig. GWA results for all exogenous reads.** Manhattan plots, enrichment of *a priori* candidate
600 variants and QQplots for all exogenous reads. The genome-wide significance (horizontal red lines),
601 was calculated based on unlinked variants (53), the blue line corresponds to -log(p) =5. The top
602 variants are labeled with the neighboring genes potentially affecting *exogenous reads* load.

603 **S4 Fig. Lengths and genomic locations of Differentially Methylated Regions (DMRs).** (A) DMRs
604 length distributions in different sequence contexts. (B) Numbers of hypermethylated and
605 hypomethylated DMRs in each genomic feature.

606 **S5 Fig. EWA enrichment in different genomic features and *P*-value distributions.** (A) Enrichment of
607 associations in different genomic features for increasing -log(p) thresholds, compared to
608 expectations from all cytosines. (B) *P*-value distributions of EWA. (C) Complement to Fig 4D showing
609 CHG and CHH methylation upstream and above the gene *MPKKK20*.

610 **S1 Table. Classification of reads.** Total reads, duplication rates, deduplicated raw reads, target,
611 ambiguous and exogenous reads and MG-RAST reads passing QC.

612 **S2 Table. MG-RAST classification of exogenous reads.** Results of MG-RAST classification of
613 exogenous reads at the family level, using RefSeq as query database.

614 **S3 Table. Competitive mapping pseudo-reference for aphid identification.** Fasta file combining
615 mitochondrial sequences of *B. Brassicaceae, A. pisum* and *M. persicae*, with structural variants
616 removed.

617 **S4 Table. Competitive mapping pseudo-reference for mildew identification.** Fasta file combining
618 ITS sequences of *Blumeria graminis* and *Erysiphe cruciferarum*, with structural variants removed.

619 **S5 Table. Results of competitive mapping for pest identification.** Number of reads mapping
620 uniquely to the pseudo-reference genomes of different aphid (mitochondrial DNA for either *B.*
621 *Brassicaceae, A. pisum* or *M. persicae*) or mildew species (ITS sequence for either *B. graminis* or *E.*
622 *cruciferaum*).

623 **S6 Table. Exogenous reads used for downstream analyses.** Classes of exogenous reads used in the
624 analyses, including the nine groups from MG-RAST and two from mapping to the *M. persicae* and *B.*
625 *aphidicola* reference genomes.

626 **S7 Table. Quantification of glucosinolates.** Glucosinolate concentrations in leaves of *T. arvense*,
627 obtained from offspring of the sequenced plants, not infested by any herbivores nor pathogens.

628 **S8 Table. *A priori* "defense response" candidate genes used for the GWA enrichment analysis.** List
629 of *T. arvense* candidate genes used for the GWA enrichment analysis: orthologs of *A. thaliana* genes
630 annotated with the GO term "defense response".

631 **S9 Table. Differentially Methylated Regions based on *M. persicae* load.** List of DMRs called
632 between the 20 samples with the highest and the lowest *M. persicae* load.

S10 Table. Differentially Methylated Regions based on Erysiphales load. List of DMRs called between the 20 samples with the highest and the lowest Erysiphales load.

Code and data availability statement

The seed material from the sequenced lines is available at the Nottingham Arabidopsis Stock Centre (NASC) under stock numbers N950001 to 950204. Genomic and bisulfite sequencing raw data are available on the ENA Sequence Read Archive (www.ebi.ac.uk/ena/) under study accession number PRJEB50950. The reference genome and annotations were previously published by Nunn et al. (2022) (29). GWA and EWA results in a format compatible with the Integrative Genomics Viewer (https://www.igv.org/) are available on Zenodo (https://zenodo.org/records/10011535).

All code used in this study is available and documented on GitHub. The scripts for variant calling, filtering and imputation are on https://github.com/Dario-Galanti/BinAC_varcalling, and the scripts for the classification of sequencing reads and MG-RAST analysis are in https://github.com/Dario-Galanti/Exoreads_treasure and https://github.com/junhee-jung/MG-RAST-read-counter respectively. The pipelines for methylation and DMR calling from WGBS data can be found on the EpiDiverse GitHub (https://github.com/EpiDiverse). The workflow for downstream analysis of methylation data is on https://github.com/Dario-Galanti/WGBS_downstream/tree/main/WGBS_simpleworkflow. Finally, the scripts for running GWA and EWA analysis are on https://github.com/Dario-Galanti/multipheno_GWAS/tree/main/gemmaGWAS and https://github.com/Dario-Galanti/EWAS/tree/main/gemmaEWAS respectively.

Funding

This work was supported by the EU Horizon 2020 program under Marie Skłodowska-Curie grant agreement 764965 (Innovative Training Network EpiDiverse; https://epidiverse.eu; PhD fellowship of DG), as well as by the Deutsche Forschungsgemeinschaft (DFG) as part of the priority programme 2125 Deconstruction and Reconstruction of the Plant Microbiota, “DECRyPT” (grant 401829393 to OB; PhD fellowship of JHJ). The funders had no role in study design, data collection and analysis, decision to publish, or preparation of the manuscript.

Acknowledgments

We thank the EpiDiverse network for its amazing support and discussions, in particular Adrián Contreras-Garrido, Bárbara Díez Rodríguez, Iris Sammarco, Adam Nunn, Daniela Ramos and Anupoma Troyee for their close collaboration. We also thank Frank Reis for his feedback and expert tips for the project, and Cecilia Heyworth for proofreading the manuscript. We thank Peter Stadler at the University of Leipzig and David Langenberger from ecSeq, which helped with computing and hosted the EpiDiverse servers. The BinAC cluster is managed by the High Performance and Cloud Computing Group at the Zentrum für Datenverarbeitung of the University of Tübingen, and supported by the state of Baden-Württemberg through bwHPC and the German Research Foundation (DFG) through grant no INST 37/935-1 FUGG.

Author Contributions

Dario Galanti: Conceptualization, Methodology, Formal analysis, Investigation, Data Curation, Writing – Original Draft Preparation, Visualization.

Jun Hee Jung: Conceptualization, Methodology, Data Curation, Writing – Review & Editing.

Caroline Müller: Investigation, Writing – Review & Editing.

Oliver Bossdorf: Conceptualization, Methodology, Writing – Original Draft Preparation, Supervision, Funding Acquisition.

References

1. Züst T, Heichinger C, Grossniklaus U, Harrington R, Kliebenstein DJ, Turnbull LA. Natural Enemies Drive Geographic Variation in Plant Defenses. Science. 2012 Oct 5; 338(6103):116–9. https://www.science.org/doi/full/10.1126/science.1226397

2. Kerwin R, Feusier J, Corwin J, Rubin M, Lin C, Muok A, et al. Natural genetic variation in Arabidopsis thaliana defense metabolism genes modulates field fitness. Kant MR, editor. eLife. 2015 Apr 13; 4:e05604. https://doi.org/10.7554/eLife.05604

3. Chan EKF, Rowe HC, Kliebenstein DJ. Understanding the Evolution of Defense Metabolites in Arabidopsis thaliana Using Genome-wide Association Mapping. Genetics. 2010 Jul 1; 185(3):991–1007. https://doi.org/10.1534/genetics.109.108522

692 4. Corwin JA, Copeland D, Feusier J, Subedy A, Eshbaugh R, Palmer C, et al. The Quantitative Basis of the
693 Arabidopsis Innate Immune System to Endemic Pathogens Depends on Pathogen Genetics. PLOS Genet.
694 2016 Feb 11; 12(2):e1005789.
695 https://journals.plos.org/plosgenetics/article?id=10.1371/journal.pgen.1005789

696 5. Thoen MPM, Olivas NHD, Kloth KJ, Coolen S, Huang PP, Aarts MGM, et al. Genetic architecture of plant
697 stress resistance: multi-trait genome-wide association mapping. New Phytol. 2017; 213(3):1346–62.
698 https://nph.onlinelibrary.wiley.com/doi/abs/10.1111/nph.14220

699 6. Hanson AA, Lorenz AJ, Hesler LS, Bhusal SJ, Bansal R, Michel AP, et al. Genome-Wide Association Mapping
700 of Host-Plant Resistance to Soybean Aphid. Plant Genome. 2018; 11(3):180011.
701 https://acsess.onlinelibrary.wiley.com/doi/abs/10.3835/plantgenome2018.02.0011

702 7. Jaouannet M, Morris JA, Hedley PE, Bos JIB. Characterization of Arabidopsis Transcriptional Responses to
703 Different Aphid Species Reveals Genes that Contribute to Host Susceptibility and Non-host Resistance.
704 PLOS Pathog. 2015 mag; 11(5):e1004918.
705 https://journals.plos.org/plospathogens/article?id=10.1371/journal.ppat.1004918

706 8. Geng S, Kong X, Song G, Jia M, Guan J, Wang F, et al. DNA methylation dynamics during the interaction of
707 wheat progenitor Aegilops tauschii with the obligate biotrophic fungus Blumeria graminis f. sp. tritici. New
708 Phytol. 2019; 221(2):1023–35. https://onlinelibrary.wiley.com/doi/abs/10.1111/nph.15432

709 9. Annacondia ML, Markovic D, Reig-Valiente JL, Scaltsoyiannes V, Pieterse CMJ, Ninkovic V, et al. Aphid
710 feeding induces the relaxation of epigenetic control and the associated regulation of the defense
711 response in Arabidopsis. New Phytol. 2021; 230(3):1185–200.
712 https://nph.onlinelibrary.wiley.com/doi/abs/10.1111/nph.17226

713 10. Kinoshita T, Seki M. Epigenetic Memory for Stress Response and Adaptation in Plants. Plant Cell Physiol.
714 2014 Nov 1; 55(11):1859–63. https://academic.oup.com/pcp/article/55/11/1859/2756009

715 11. Espinas NA, Saze H, Saijo Y. Epigenetic Control of Defense Signaling and Priming in Plants. Front Plant Sci.
716 2016 Aug 11; 7:1201. https://www.ncbi.nlm.nih.gov/pmc/articles/PMC4980392/

717 12. Lämke J, Bäurle I. Epigenetic and chromatin-based mechanisms in environmental stress adaptation and
718 stress memory in plants. Genome Biol. 2017 Jun 27; 18(1):124. https://doi.org/10.1186/s13059-017-1263-
719 6

720 13. He Y, Li Z. Epigenetic Environmental Memories in Plants: Establishment, Maintenance, and
721 Reprogramming. Trends Genet. 2018 Aug 22;
722 http://www.sciencedirect.com/science/article/pii/S0168952518301276

723 14. Roquis D, Robertson M, Yu L, Thieme M, Julkowska M, Bucher E. Genomic impact of stress-induced
724 transposable element mobility in Arabidopsis. Nucleic Acids Res. 2021 Oct 11; 49(18):10431–47.
725 https://doi.org/10.1093/nar/gkab828

726 15. Law JA, Jacobsen SE. Establishing, maintaining and modifying DNA methylation patterns in plants and
727 animals. Nat Rev Genet. 2010 Mar; 11(3):204–20. https://www.nature.com/articles/nrg2719

728 16. Zhang H, Lang Z, Zhu JK. Dynamics and function of DNA methylation in plants. Nat Rev Mol Cell Biol. 2018
729 May 21; 1. https://www.nature.com/articles/s41580-018-0016-z

730 17. Liu J, He Z. Small DNA Methylation, Big Player in Plant Abiotic Stress Responses and Memory. Front Plant
731 Sci. 2020; 11. https://www.frontiersin.org/article/10.3389/fpls.2020.595603

732 18. Wojtaszek P. Oxidative burst: an early plant response to pathogen infection. Biochem J. 1997 Mar 15;
733 322(Pt 3):681–92. https://www.ncbi.nlm.nih.gov/pmc/articles/PMC1218243/

734 19. War AR, Paulraj MG, Ahmad T, Buhroo AA, Hussain B, Ignacimuthu S, et al. Mechanisms of plant defense
735 against insect herbivores. Plant Signal Behav. 2012 Oct 1; 7(10):1306–20.
736 https://doi.org/10.4161/psb.21663

737 20. Kant MR, Jonckheere W, Knegt B, Lemos F, Liu J, Schimmel BCJ, et al. Mechanisms and ecological
738 consequences of plant defence induction and suppression in herbivore communities. Ann Bot. 2015 Jun 1;
739 115(7):1015–51. https://doi.org/10.1093/aob/mcv054

740 21. Melotto M, Zhang L, Oblessuc PR, He SY. Stomatal Defense a Decade Later. Plant Physiol . 2017 Jun 1;
741 174(2):561–71. https://doi.org/10.1104/pp.16.01853

742 22. Muhammad T, Zhang F, Zhang Y, Liang Y. RNA Interference: A Natural Immune System of Plants to
743 Counteract Biotic Stressors. Cells. 2019 Jan; 8(1):38. https://www.mdpi.com/2073-4409/8/1/38

744 23. Kutyniok M, Müller C. Crosstalk between above- and belowground herbivores is mediated by minute
745 metabolic responses of the host Arabidopsis thaliana. J Exp Bot. 2012 Oct 1; 63(17):6199–210.
746 https://doi.org/10.1093/jxb/ers274

747 24. Nalam V, Louis J, Patel M, Shah J. Arabidopsis-Green Peach Aphid Interaction: Rearing the Insect, No-
748 choice and Fecundity Assays, and Electrical Penetration Graph Technique to Study Insect Feeding
749 Behavior. Bio-Protoc. 2018 Aug 5; 8(15):e2950.

750 25. Sangiovanni M, Granata I, Thind AS, Guarracino MR. From trash to treasure: detecting unexpected
751 contamination in unmapped NGS data. BMC Bioinformatics. 2019 Apr 18; 20(4):168.
752 https://doi.org/10.1186/s12859-019-2684-x

753 26. Roman-Reyna V, Pinili D, Borja FN, Quibod IL, Groen SC, Alexandrov N, et al. Characterization of the Leaf
754 Microbiome from Whole-Genome Sequencing Data of the 3000 Rice Genomes Project. Rice. 2020 Oct 9;
755 13(1):72. https://doi.org/10.1186/s12284-020-00432-1

756 27. Gathercole LAP, Nocchi G, Brown N, Coker TLR, Plumb WJ, Stocks JJ, et al. Evidence for the Widespread
757 Occurrence of Bacteria Implicated in Acute Oak Decline from Incidental Genetic Sampling. Forests. 2021
758 Dec; 12(12):1683. https://www.mdpi.com/1999-4907/12/12/1683

759 28. Geng Y, Guan Y, Qiong L, Lu S, An M, Crabbe MJC, et al. Genomic analysis of field pennycress (*Thlaspi*
760 *arvense*) provides insights into mechanisms of adaptation to high elevation. BMC Biol. 2021 Jul 22;
761 19(1):143. https://doi.org/10.1186/s12915-021-01079-0

762 29. Nunn A, Rodríguez-Arévalo I, Tandukar Z, Frels K, Contreras-Garrido A, Carbonell-Bejerano P, et al.
763 Chromosome-level *Thlaspi arvense* genome provides new tools for translational research and for a newly
764 domesticated cash cover crop of the cooler climates. Plant Biotechnol J. 2022.
765 https://onlinelibrary.wiley.com/doi/abs/10.1111/pbi.13775

766 30. Hu Y, Wu X, Jin G, Peng J, Leng R, Li L, et al. Rapid Genome Evolution and Adaptation of Thlaspi arvense
767 Mediated by Recurrent RNA-Based and Tandem Gene Duplications. Front Plant Sci. 2022; 12.
768 https://www.frontiersin.org/articles/10.3389/fpls.2021.772655

769 31. Troyee AN, Medrano M, Müller C, Alonso C. Variation in DNA methylation and response to short-term
770 herbivory in Thlaspi arvense. Flora. 2022 Aug 1; 293:152106.
771 https://www.sciencedirect.com/science/article/pii/S0367253022001037

772 32. Galanti D, Ramos-Cruz D, Nunn A, Rodríguez-Arévalo I, Scheepens JF, Becker C, et al. Genetic and
773 environmental drivers of large-scale epigenetic variation in Thlaspi arvense. PLOS Genet. 2022 ott;
774 18(10):e1010452. https://journals.plos.org/plosgenetics/article?id=10.1371/journal.pgen.1010452

775 33. Dorn KM, Fankhauser JD, Wyse DL, Marks MD. A draft genome of field pennycress (*Thlaspi arvense*)
776 provides tools for the domestication of a new winter biofuel crop. DNA Res. 2015 Apr 1; 22(2):121–31.
777 https://academic.oup.com/dnaresearch/article/22/2/121/332636

778 34. Frels K, Chopra R, Dorn KM, Wyse DL, Marks MD, Anderson JA. Genetic Diversity of Field Pennycress
779 (*Thlaspi arvense*) Reveals Untapped Variability and Paths Toward Selection for Domestication. Agronomy.
780 2019 Jun; 9(6):302. https://www.mdpi.com/2073-4395/9/6/302

781 35. Chopra R, Johnson EB, Emenecker R, Cahoon EB, Lyons J, Kliebenstein DJ, et al. Progress toward the
782 identification and stacking of crucial domestication traits in pennycress. Plant Biology; 2019 Apr.
783 http://biorxiv.org/lookup/doi/10.1101/609990

784 36. Zhao R, Yang X, Li M, Peng X, Wei M, Zhang X, et al. Biodiesel preparation from Thlaspi arvense L. seed oil
785 utilizing a novel ionic liquid core-shell magnetic catalyst. Ind Crops Prod. 2021 Apr 1; 162:113316.
786 https://www.sciencedirect.com/science/article/pii/S0926669021000807

787 37. Kajiya-Kanegae H, Nagasaki H, Kaga A, Hirano K, Ogiso-Tanaka E, Matsuoka M, et al. Whole-genome
788 sequence diversity and association analysis of 198 soybean accessions in mini-core collections. DNA Res.
789 2021 Feb 1; 28(1):dsaa032. https://doi.org/10.1093/dnares/dsaa032

790 38. Colgan TJ, Arce AN, Gill RJ, Ramos Rodrigues A, Kanteh A, Duncan EJ, et al. Genomic Signatures of Recent
791 Adaptation in a Wild Bumblebee. Mol Biol Evol. 2022 Feb 1; 39(2):msab366.
792 https://doi.org/10.1093/molbev/msab366

793 39. Habyarimana E, Gorthy S, Baloch FS, Ercisli S, Chung G. Whole-genome resequencing of Sorghum bicolor
794 and S. bicolor × S. halepense lines provides new insights for improving plant agroecological characteristics.
795 Sci Rep. 2022 Apr 1; 12(1):5556. https://www.nature.com/articles/s41598-022-09433-0

796 40. Mekbib Y, Tesfaye K, Dong X, Saina JK, Hu GW, Wang QF. Whole-genome resequencing of Coffea arabica
797 L. (Rubiaceae) genotypes identify SNP and unravels distinct groups showing a strong geographical pattern.
798 BMC Plant Biol. 2022 Feb 14; 22(1):69. https://doi.org/10.1186/s12870-022-03449-4

799 41. Metheringham CL, Plumb WJ, Stocks JJ, Kelly LJ, Gorriz MN, Moat J, et al. Rapid polygenic adaptation in a
800 wild population of ash trees under a novel fungal epidemic. bioRxiv; 2022. p. 2022.08.01.502033.
801 https://www.biorxiv.org/content/10.1101/2022.08.01.502033v3

802 42. Nocchi G, Brown N, Coker TLR, Plumb WJ, Stocks JJ, Denman S, et al. Genomic structure and diversity of
803 oak populations in British parklands. PLANTS PEOPLE PLANET. 2022; 4(2):167–81.
804 https://onlinelibrary.wiley.com/doi/abs/10.1002/ppp3.10229

805 43. Friis G, Smith EG, Lovelock CE, Ortega A, Marshell A, Duarte CM, et al. Rapid diversification of grey
806 mangroves (Avicennia marina) driven by geographic isolation and extreme environmental conditions in
807 the Arabian Peninsula. Mol Ecol. 2024;33(4):e17260.
808 https://onlinelibrary.wiley.com/doi/full/10.1111/mec.17260

809 44. Meyer F, Paarmann D, D'Souza M, Olson R, Glass E, Kubal M, et al. The metagenomics RAST server – a
810 public resource for the automatic phylogenetic and functional analysis of metagenomes. BMC
811 Bioinformatics. 2008 Sep 19; 9(1):386. https://doi.org/10.1186/1471-2105-9-386

812 45. Keegan KP, Glass EM, Meyer F. MG-RAST, a Metagenomics Service for Analysis of Microbial Community
813 Structure and Function. Methods Mol Biol Clifton NJ. 2016;1399:207–33.

46. CABI. Myzus persicae (green peach aphid). CABI Compend . 2021 Dec 18 [cited 2023 Apr 7];CABI Compendium:35642. https://www.cabidigitallibrary.org/doi/10.1079/cabicompendium.35642

47. Gabryś B, Pawluk M. Acceptability of different species of Brassicaceae as hosts for the cabbage aphid. Entomol Exp Appl. 1999; 91(1):105–9. https://onlinelibrary.wiley.com/doi/abs/10.1046/j.1570-7458.1999.00471.x

48. Warwick SI, Francis A, Susko DJ. The biology of Canadian weeds. 9. Thlaspi arvense L. (updated). Can J Plant Sci. 2002 Oct 1; 82(4):803–23. http://www.nrcresearchpress.com/doi/abs/10.4141/P01-159

49. Feuerborn TR, Palkopoulou E, van der Valk T, von Seth J, Munters AR, Pečnerová P, et al. Competitive mapping allows for the identification and exclusion of human DNA contamination in ancient faunal genomic datasets. BMC Genomics. 2020 Nov 30; 21(1):844. https://doi.org/10.1186/s12864-020-07229-y

50. Singh KS, Cordeiro EMG, Troczka BJ, Pym A, Mackisack J, Mathers TC, et al. Global patterns in genomic diversity underpinning the evolution of insecticide resistance in the aphid crop pest Myzus persicae. Commun Biol. 2021 Jul 7; 4(1):1–16. https://www.nature.com/articles/s42003-021-02373-x

51. Kruijer, Willem, and with a contribution from Ian White, contains data collected by Padraic Flood and Rik Kooke. 2019. "Heritability: Marker-Based Estimation of Heritability Using Individual Plant or Plot Data." https://CRAN.R-project.org/package=heritability.

52. Gao J, Fang C, Zhao B. The latitudinal herbivory hypothesis revisited: To be part is to be whole. Ecol Evol. 2019; 9(7):3681–8. https://onlinelibrary.wiley.com/doi/abs/10.1002/ece3.2759

53. Atwell S, Huang YS, Vilhjálmsson BJ, Willems G, Horton M, Li Y, et al. Genome-wide association study of 107 phenotypes in Arabidopsis thaliana inbred lines. Nature. 2010 Jun; 465(7298):627–31. https://www.nature.com/articles/nature08800

54. Sobota RS, Shriner D, Kodaman N, Goodloe R, Zheng W, Gao YT, et al. Addressing population-specific multiple testing burdens in genetic association studies. Ann Hum Genet. 2015 Mar; 79(2):136–47. https://www.ncbi.nlm.nih.gov/pmc/articles/PMC4334751/

55. Kim JH, Jander G. Myzus persicae (green peach aphid) feeding on Arabidopsis induces the formation of a deterrent indole glucosinolate. Plant J. 2007; 49(6):1008–19. https://onlinelibrary.wiley.com/doi/abs/10.1111/j.1365-313X.2006.03019.x

56. Klingauf F, Şengonca Ç, Bennewitz H. Einfluß von Sinigrin auf die Nahrungsaufnahme polyphager und oligophager Blattlausarten (Aphididae) (Effect of Sinigrin on Sucrose Uptake by Some Polyphagous and Oligophagous Aphids (Aphididae)). Oecologia. 1972; 9(1):53–7. https://www.jstor.org/stable/4214736

844 57. The Arabidopsis Information Resource (TAIR). 2000.
845 www.arabidopsis.org/servlets/TairObject?id=137911&type=locus

846 58. Camacho C, Coulouris G, Avagyan V, Ma N, Papadopoulos J, Bealer K, et al. BLAST+: architecture and
847 applications. BMC Bioinformatics. 2009 Dec 15; 10(1):421. https://doi.org/10.1186/1471-2105-10-421

848 59. Martin M. Cutadapt removes adapter sequences from high-throughput sequencing reads. EMBnet.journal
849 . 2011 May 2 [cited 2021 Dec 2];17(1):10–2.
850 http://journal.embnet.org/index.php/embnetjournal/article/view/200

851 60. Andrews S. FASTQC. A quality control tool for high throughput sequence data | BibSonomy. 2010 [cited
852 2023 Feb 13]. https://www.bioinformatics.babraham.ac.uk/projects/fastqc/

853 61. Ewels P, Magnusson M, Lundin S, Käller M. MultiQC: summarize analysis results for multiple tools and
854 samples in a single report. Bioinformatics. 2016 Oct 1 [cited 2023 Feb 13];32(19):3047–8.
855 https://doi.org/10.1093/bioinformatics/btw354

856 62. Li H, Durbin R. Fast and accurate short read alignment with Burrows–Wheeler transform. Bioinformatics.
857 2009 Jul 15 [cited 2021 Jun 11]; 25(14):1754–60. https://doi.org/10.1093/bioinformatics/btp324

858 63. Van der Auwera GA, Carneiro MO, Hartl C, Poplin R, Angel G del, Levy-Moonshine A, et al. From FastQ
859 Data to High-Confidence Variant Calls: The Genome Analysis Toolkit Best Practices Pipeline. Curr Protoc
860 Bioinforma. 2013; 43(1):11.10.1-11.10.33.
861 https://currentprotocols.onlinelibrary.wiley.com/doi/abs/10.1002/0471250953.bi1110s43

862 64. Poplin R, Ruano-Rubio V, DePristo MA, Fennell TJ, Carneiro MO, Auwera GAV der, et al. Scaling accurate
863 genetic variant discovery to tens of thousands of samples. bioRxiv. 2018 Jul 24;201178.
864 https://www.biorxiv.org/content/10.1101/201178v3

865 65. Frantzeskakis L, Kracher B, Kusch S, Yoshikawa-Maekawa M, Bauer S, Pedersen C, et al. Signatures of host
866 specialization and a recent transposable element burst in the dynamic one-speed genome of the fungal
867 barley powdery mildew pathogen. BMC Genomics. 2018 May 22; 19(1):381.
868 https://doi.org/10.1186/s12864-018-4750-6

869 66. Danecek P, Bonfield JK, Liddle J, Marshall J, Ohan V, Pollard MO, et al. Twelve years of SAMtools and
870 BCFtools. GigaScience. 2021 Feb 1 [cited 2022 Aug 15]; 10(2):giab008.
871 https://doi.org/10.1093/gigascience/giab008

872 67. Danecek P, Auton A, Abecasis G, Albers CA, Banks E, DePristo MA, et al. The variant call format and
873 VCFtools. Bioinformatics. 2011 Aug 1; 27(15):2156–8. https://doi.org/10.1093/bioinformatics/btr330

874 68. Browning BL, Zhou Y, Browning SR. A One-Penny Imputed Genome from Next-Generation Reference
875 Panels. Am J Hum Genet. 2018 Sep 6 [cited 2021 Jun 11]; 103(3):338–48.
876 https://www.sciencedirect.com/science/article/pii/S0002929718302428

877 69. Paczian T, Trimble WL, Gerlach W, Harrison T, Wilke A, Meyer F. The MG-RAST API explorer: an on-ramp
878 for RESTful query composition. BMC Bioinformatics. 2019 Nov 8 [cited 2023 Apr 19]; 20(1):561.
879 https://doi.org/10.1186/s12859-019-2993-0

880 70. Robinson KM, Hawkins AS, Santana-Cruz I, Adkins RS, Shetty AC, Nagaraj S, et al. Aligner optimization
881 increases accuracy and decreases compute times in multi-species sequence data. Microb Genomics. 2017
882 Jul 8; 3(9):e000122. https://www.ncbi.nlm.nih.gov/pmc/articles/PMC5643015/

883 71. Prince D, Mugford S, Vincent T, Hogenhout S. Pea Aphid Survival Assays on Arabidopsis thaliana. BIO-
884 Protoc. 2014 [cited 2023 Oct 11]; 4(19). https://bio-protocol.org/e1251

885 72. National Center for Biotechnology Information (NCBI). Bethesda (MD): National Library of Medicine (US).
886 1988. NCBI. https://www.ncbi.nlm.nih.gov/

887 73. Sievers F, Wilm A, Dineen D, Gibson TJ, Karplus K, Li W, et al. Fast, scalable generation of high-quality
888 protein multiple sequence alignments using Clustal Omega. Mol Syst Biol. 2011 Jan [cited 2023 Oct 12];
889 7(1):539. https://www.embopress.org/doi/full/10.1038/msb.2011.75

890 74. Agerbirk N, Olsen CE, Heimes C, Christensen S, Bak S, Hauser TP. Multiple hydroxyphenethyl glucosinolate
891 isomers and their tandem mass spectrometric distinction in a geographically structured polymorphism in
892 the crucifer Barbarea vulgaris. Phytochemistry. 2015 Jul 1; 115:130–42.
893 https://www.sciencedirect.com/science/article/pii/S0031942214003665

894 75. Copernicus Climate Change Service. E-OBS daily gridded meteorological data for Europe from 1950 to
895 present derived from in-situ observations. ECMWF; 2020 [cited 2022 Feb 9].
896 https://cds.climate.copernicus.eu/doi/10.24381/cds.151d3ec6

897 76. Ziyatdinov A, Vázquez-Santiago M, Brunel H, Martinez-Perez A, Aschard H, Soria JM. lme4qtl: linear mixed
898 models with flexible covariance structure for genetic studies of related individuals. BMC Bioinformatics.
899 2018 Feb 27 [cited 2022 Feb 1]; 19(1):68. https://doi.org/10.1186/s12859-018-2057-x

900 77. Zhou X, Stephens M. Genome-wide efficient mixed-model analysis for association studies. Nat Genet.
901 2012 Jul; 44(7):821–4. https://www.nature.com/articles/ng.2310

902 78. Purcell S, Neale B, Todd-Brown K, Thomas L, Ferreira MAR, Bender D, et al. PLINK: A Tool Set for Whole-
903 Genome Association and Population-Based Linkage Analyses. Am J Hum Genet. 2007 Sep 1 [cited 2021 Jun
904 17]; 81(3):559–75. https://www.sciencedirect.com/science/article/pii/S0002929707613524

905 79. Emms DM, Kelly S. OrthoFinder: phylogenetic orthology inference for comparative genomics. Genome
906 Biol. 2019 Nov 14 [cited 2021 Jul 31]; 20(1):238. https://doi.org/10.1186/s13059-019-1832-y

907 80. Nordborg M, Hu TT, Ishino Y, Jhaveri J, Toomajian C, Zheng H, et al. The Pattern of Polymorphism in
908 Arabidopsis thaliana. PLOS Biology. 2005 May 24;3(7):e196.
909 https://doi.org/10.1371/journal.pbio.0030196.

910 81. Nunn A, Can SN, Otto C, Fasold M, Díez Rodríguez B, Fernández-Pozo N, et al. EpiDiverse Toolkit: a
911 pipeline suite for the analysis of bisulfite sequencing data in ecological plant epigenetics. NAR Genomics
912 Bioinforma. 2021 Dec 1; 3(4):lqab106. https://doi.org/10.1093/nargab/lqab106

913 82. Quinlan AR, Hall IM. BEDTools: a flexible suite of utilities for comparing genomic features. Bioinformatics.
914 2010 Mar 15; 26(6):841–2. https://doi.org/10.1093/bioinformatics/btq033

915